Journal of the American College of Cardiology Vol. 50, No. 1, 2007

Published by Elsevier Inc.
ISSN 0735-1097/07/$32.00
doi:10.1016/j.jacc.2007.02.066

Ganglionated Plexi Modulate Extrinsic Cardiac Autonomic Nerve Input

Effects on Sinus Rate, Atrioventricular Conduction, Refractoriness, and Inducibility of Atrial Fibrillation

Yinglong Hou, MD,* Benjamin J. Scherlag, PHD,† Jiaxiong Lin, MD,† Ying Zhang, MD, PHD,‡ Zhibing Lu, MD,† Kim Truong, DO,† Eugene Patterson, PHD,† Ralph Lazzara, MD,† Warren M. Jackman, MD,† Sunny S. Po, MD, PHD†

Shandong, China; and Oklahoma City, Oklahoma

Objectives This study sought to systematically investigate the interactions between the extrinsic and intrinsic cardiac autonomic nervous system (ANS) in modulating electrophysiological properties and atrial fibrillation (AF) initiation.

Background Systematic ganglionated plexi (GP) ablation to evaluate the extrinsic and intrinsic cardiac ANS relationship has not been detailed.

Methods The following GP were exposed in 28 dogs: anterior right GP (ARGP) near the sinoatrial node, inferior right ganglionated plexi (IRGP) at the junction of the inferior vena cava and atria, and superior left ganglionated plexi (SLGP) near the junction of left superior pulmonary vein and left pulmonary artery. With unilateral vagosympathetic trunk stimulation (0.6 to 8.0 V, 20 Hz, 0.1 ms in duration), sinus rate (SR), and ventricular rate (VR) during AF were compared before and after sequential ablation of SLGP, ARGP, and IRGP.

Results The SLGP ablation significantly attenuated the SR and VR slowing responses with right or left vagosympathetic trunk stimulation. Subsequent ARGP ablation produced additional effects on SR slowing but not VR slowing. After SLGP + ARGP ablation, IRGP ablation eliminated VR slowing but did not further attenuate SR slowing with vagosympathetic trunk stimulation. Unilateral right and left vagosympathetic trunk stimulation shortened the effective refractory period and increased AF inducibility of atrium and pulmonary vein near the ARGP and SLGP, respectively. The ARGP ablation eliminated ERP shortening and AF inducibility with right vagosympathetic trunk stimulation, whereas SLGP ablation eliminated ERP shortening but not AF inducibility with left vagosympathetic trunk stimulation.

Conclusions The GP function as the "integration centers" that modulate the autonomic interactions between the extrinsic and intrinsic cardiac ANS. This interaction is substantially more intricate than previously thought. (J Am Coll Cardiol 2007;50:61–8) © 2007 by the American College of Cardiology Foundation

Autonomic innervation of the heart involves both the extrinsic and the intrinsic cardiac autonomic nervous system (ANS). The former collectively includes the ganglia in the brain or along the spinal cord and their axons (e.g., the vagosympathetic trunk) en route to the heart; the latter consists of the autonomic ganglia and axons located on the heart itself or along the great vessels in the thorax (1). Ample structural and functional evidence indicates that the intrinsic cardiac ANS forms a complex neural network composed of ganglionated plexi (GP) concentrated within epicardial fat pads and the interconnecting ganglia and axons (2–5).

Basic and clinical studies on atrial fibrillation (AF) resulting from changes in the ANS have underscored the contributions from the extrinsic cardiac ANS, mainly by stimulating the vagosympathetic trunk in animals (5,6) or by observing the pattern of AF initiation in patients (7). Recently, stimulation of the intrinsic cardiac ANS by applying high-frequency electrical stimulation to the GP (8) or by injecting parasympathomimetics into the GP (9) has drawn attention to the critical role of the intrinsic cardiac ANS in the dynamics of AF initiation and maintenance. How the extrinsic and intrinsic cardiac ANS operate cooperatively in regard to these aspects has not been detailed. The purpose of this study was to systemically

From the *Department of Cardiology, Shandong Provincial Qianfoshan Hospital, Clinical Medical College of Shandong University, Jinan City, Shandong, China; and the †Cardiac Arrhythmia Research Institute, College of Medicine, and ‡Center for American Indian Health Research, College of Public Health, University of Oklahoma Health Sciences Center, Oklahoma City, Oklahoma. Supported by grant 0650077Z from the American Heart Association (to Dr. Po) and grant 5K23HL069972 from the National Heart, Lung, and Blood Institute (to Dr. Po).

Manuscript received October 10, 2006; revised manuscript received February 12, 2007, accepted February 27, 2007.

JACC Vol. 50, No. 1, 2007
July 3, 2007:61–8

Abbreviations and Acronyms

AF = atrial fibrillation
ANS = autonomic nervous system
ARGP = anterior right ganglionated plexi
ERP = effective refractory period
GP = ganglionated plexi
IRGP = inferior right ganglionated plexi
LSPV = left superior pulmonary vein
RSPV = right superior pulmonary vein
SA = sinoatrial
SLGP = superior left ganglionated plexi
SR = sinus rate
VR = ventricular rate

investigate the interactions between the extrinsic and intrinsic cardiac ANS in the context of modulating sinus and atrioventricular (AV) nodal function and facilitating AF inducibility.

Methods

All animal studies were reviewed and approved by the Institutional Animal Care and Use Committee of the University of Oklahoma Health Sciences Center. Twenty-eight adult mongrel dogs weighing 20 to 25 kg were anesthetized with sodium pentobarbital, 50 mg/kg, and ventilated with room air by a positive pressure respirator. Standard electrocardiographic leads II and aVR were continuously monitored. Core body temperature was maintained at 36.5°C ± 1.5°C. All recordings were displayed on a Bard Computerized Electrophysiology system (Bard, Billerica, Massachusetts).

Autonomic stimulation. Both cervical vagosympathetic trunks were exposed by dissections. A pair of Teflon-coated silver wires (0.1-mm diameter) was inserted into the cervical vagosympathetic trunks for stimulation. Vagosympathetic stimulation was performed by applying high-frequency electrical stimulation (20 Hz, 0.1 ms duration, square waves, 0.6 to 8.0 V) to each of the vagosympathetic trunk via a stimulator (Grass-S88, Astro-Med; West Warwick, Rhode Island). A right thoracotomy at the 4th intercostal space was performed to expose the fat pad containing the anterior right GP (ARGP) situated between the caudal end of the sinoatrial (SA) node and the right superior pulmonary vein (RSPV)–atrial junction (10) (Fig. 1A). The inferior right GP (IRGP) located at the junction of the inferior vena cava and both atria was visualized by gently reflecting the inferior vena cava. A left thoracotomy at the 4th intercostal space was used to expose the superior left GP (SLGP) located adjacent to the left superior pulmonary vein (LSPV)–atrial junction between the left atrial appendage and left pulmonary artery (10) (Fig. 1B).

The GP were identified by applying high-frequency stimulation using a bipolar electrode probe (AtriCure, West Chester, Ohio) through a Grass stimulator as described above. The effects of vagosympathetic stimulation at various voltage levels on the sinus rate (SR) were determined as well as the averaged ventricular rate (VR) during induced AF. The average SR at each stimulation level was determined by averaging the last 10 sinus cycle lengths. The AF was induced and maintained by rapid atrial pacing (600 to 800 beats/min). During induced AF, the average VR was

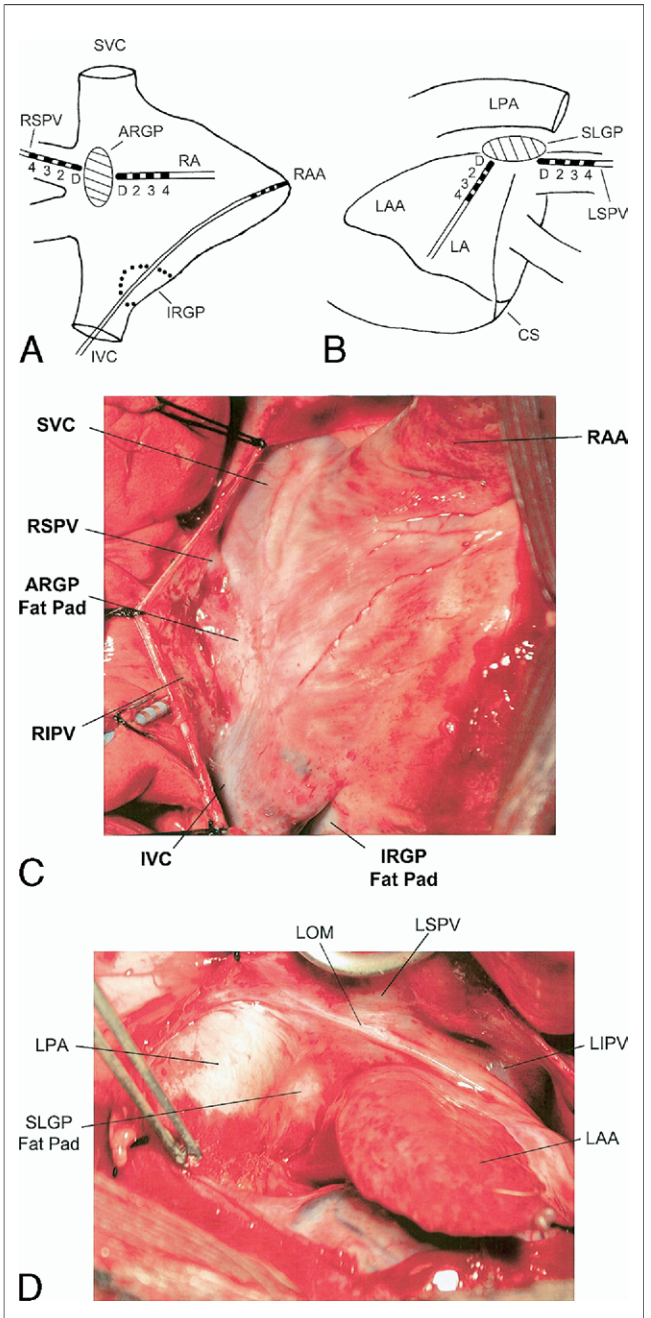

Figure 1 **Schematic and Photographic Representation of the Right and Left Thoracotomy Approach**

Schematic and photographic representation of the right **(A, C)** and left **(B, D)** atria and associated ganglionated plexi (GP). The labels **RA, RSPV, LA,** and **LSPV** indicate cardiac structures or multielectrode catheters positioned on the epicardial surface of the right atrium, right superior pulmonary veins, left atrium, and left superior pulmonary vein, respectively. For all catheters, the distal electrode pair (D,2) was positioned adjacent to the GP **(hatched area)** near the pulmonary vein–atrial junction. ARGP = anterior right ganglionated plexi; CS = coronary sinus; IRGP = inferior right ganglionated plexi; IVC = inferior vena cava; LAA = left atrial appendage; LIPV = left inferior plumonary vein; LOM = ligament of Marshall; LPA = left pulmonary artery; RAA = right atrial appendage; RIPV = right inferior pulmonary vein; SLGP = superior left ganglionated plexi; SVC = superior vena cava.

determined from the ventricular cycle lengths over the last 20 beats at each stimulation level.

To determine the interactions between extrinsic and intrinsic cardiac ANS, the SLGP, ARGP, and IRGP were ablated sequentially using the stimulation/ablation device (radiofrequency current at 460 kHz; <32.5 W; AtriCure, West Chester, Ohio). The voltages reported in this study were the delivered voltages across the catheter electrode. Completeness of GP ablation was verified by eliminating the responses (slowing of SR and VR) induced by applying maximal voltage to the GP so that positive responses were attained at much lower voltages before ablation. Identical vagosympathetic stimulation protocols as described above were applied to each vagosympathetic trunk before and after ablation of each GP.

Programmed stimulation. Programmed stimulation of myocardium was performed using a stimulator (model 5328, Medtronic, Minneapolis, Minnesota). Atrial pacing at a cycle length of 330 ms (2× diastolic threshold; threshold = 0.6 to 1.5 mA) was performed at each electrode pair of the multielectrode catheters on RA, RSPV (Fig. 1A), LA, or LSPV (Fig. 1B). Programmed electrical stimulation (starting at S1–S2 = 150 ms) was applied to each electrode pair with or without concurrent vagosympathetic stimulation (at a voltage level that reduced SR by 50%) until AF was induced or no AF was induced at maximal voltage (8.0 V). The effective refractory period (ERP) was determined at each electrode pair along the catheters positioned at RA, RSPV, LA, or LSPV before and during vagosympathetic stimulation. As the S1–S2 intervals were decreased from 150 ms to refractoriness, the longest and shortest S1–S2 interval (in ms) at which AF was induced was determined. The difference between the two was designated as the window of vulnerability (10). Thus, the mean window of vulnerability at each bipolar pair with and without served as a quantitative measure of AF inducibility.

Statistical analysis. All data are expressed as mean ± SD. The mean values of the parameters acquired during different levels of vagosympathetic stimulation were compared to the baseline state, i.e., no stimulation, using 2-way analysis of variance with time (before and after vagosympathetic stimulation) as repeated measures. The mean values of individual parameters acquired at individual level of vagosympathetic stimulation before and after GP ablation also were compared using the same statistical method. Probability values <0.05 were considered statistically significant. All analyses were conducted using SAS version 8.1 (SAS Institute Inc., Cary, North Carolina).

Results

Effects of right vagosympathetic stimulation on SR. Right vagosympathetic stimulation suppressed SR at voltage levels ≥0.6 V with a maximal effect of 90% reduction in SR (147 ± 16 beats/min baseline vs. 15 ± 19 beats/min, 8.0 V) (Table 1). We elected to ablate the SLGP first to investigate whether GP at a distance from the SA node also modulate the SR. After SLGP ablation, SR still could be slowed by right vagosympathetic stimulation (≥1.5 V) but the maximal effect was significantly attenuated to 59% (154 ± 15 beats/min baseline vs. 63 ± 35 beats/min, 8.0 V) (Table 1). The difference of SR slowing before and after SLGP ablation was statistically significant at voltage levels ≥1.5 V (P_1, Table 1). After SLGP ablation, ARGP ablation produced further attenuation of SR slowing induced by right vagosympathetic stimulation. The maximal effect was reduced to 20% (158 ± 19 beats/min baseline vs. 126 ± 16 beats/min, 8.0 V) and the differences before and after ARGP ablation also reached statistical significance at voltage levels ≥1.5 V (P_2, Table 1). Subsequent ablation of the IRGP after SLGP + ARGP ablation did not further attenuate the SR slowing effect (P_3, Table 1). Right vagosympathetic stimulation still slowed SR at voltage levels ≥1.5 V. To further examine the direction of autonomic innervation from right vagosympathetic trunk to SA node (right vagosympathetic trunk → ARGP → SLGP → SA node vs. right vagosympathetic trunk → SLGP → ARGP → SA node), only the ARGP was ablated in another 7 animals. After ARGP ablation, the magnitude of SR slowing at 8.0 V was diminished to 17% (data not shown in Tables), similar to the effects after ablation of both SLGP and ARGP (20%) (Table 1).

Effects of left vagosympathetic stimulation on SR. Left vagosympathetic stimulation produced similar but smaller

Table 1 Effects of Right Vagosympathetic Trunk Stimulation on Sinus Rate (beats/min) Before and After SLGP, ARGP, and IRGP Were Sequentially Ablated

	Baseline	0.3 V	0.6 V	1.5 V	2.4 V	3.2 V	4.5 V	8.0 V
Control, n = 10	147 ± 16	146 ± 17	113 ± 54*	37 ± 38†	25 ± 30†	20 ± 21†	15 ± 20†	15 ± 19†
SLGP ablation, n = 10	154 ± 15	154 ± 16	137 ± 26	92 ± 39†	81 ± 39†	71 ± 41†	71 ± 40†	63 ± 35†
P_1	NS	NS	NS	<0.001	<0.001	<0.001	<0.001	<0.01
SLGP + ARGP ablation, n = 10	158 ± 19	158 ± 8	148 ± 22	131 ± 17†	127 ± 16†	127 ± 17†	126 ± 16†	126 ± 16†
P_2	NS	NS	NS	<0.01	<0.001	<0.001	<0.001	<0.01
SLGP + ARGP + IRGP ablation, n = 8	149 ± 17	149 ± 16	147 ± 17	135 ± 14*	133 ± 12*	133 ± 11*	133 ± 11*	133 ± 12*
P_3	NS	NS	NS	NS	NS	NS	NS	NS

*p < 0.05; †p < 0.01 (compared with baseline).

ARGP = anterior right ganglionated plexi; baseline = no vagosympathetic stimulation; control = before ablation; IRGP = inferior right ganglionated plexi; NS = not statistically significant; P_1 = p value for comparison at each voltage level before and after SLGP ablation; P_2 = p value for comparison at each voltage level between SLGP + ARGP ablation and SLGP ablation; P_3 = p value for comparison at each voltage level between SLGP + ARGP + IRGP ablation and SLGP + ARGP ablation; SLGP = superior left ganglionated plexi.

Table 2 Effects of Left Vagosympathetic Trunk Stimulation on Sinus Rate (beats/min) Before and After SLGP, ARGP, and IRGP Were Sequentially Ablated

	Baseline	0.3 V	0.6 V	1.5 V	2.4 V	3.2 V	4.5 V	8.0 V
Control, n = 10	145 ± 18	137 ± 23	118 ± 31	78 ± 33†	71 ± 37†	66 ± 39†	65 ± 37†	63 ± 36†
SLGP ablation, n = 10	156 ± 16	155 ± 16	149 ± 16	138 ± 26	131 ± 25*	128 ± 26†	126 ± 27†	122 ± 29†
P_1	NS	<0.05	<0.01	<0.001	<0.001	<0.001	<0.001	<0.001
SLGP + ARGP ablation, n = 10	153 ± 16	153 ± 9	149 ± 14	145 ± 14	143 ± 14	142 ± 13	141 ± 12	139 ± 11*
P_2	NS	NS	NS	NS	NS	NS	NS	NS
SLGP + ARGP + IRGP ablation, n = 8	157 ± 17	157 ± 4	156 ± 17	152 ± 18	151 ± 17	149 ± 17	148 ± 17	146 ± 16
P_3	NS	NS	NS	NS	NS	NS	NS	NS

*p < 0.05; †p < 0.01 (compared with baseline).
Abbreviations as in Table 1.

effects on SR slowing compared with right vagosympathetic stimulation, with a maximal effect of 57% reduction of SR (145 ± 18 beats/min baseline vs. 63 ± 36 beats/min, 8.0 V) (Table 2). After SLGP ablation, stimulation levels ≥2.4 V still slowed SR but the maximal effect was reduced to 22% (156 ± 16 beats/min baseline vs. 122 ± 29 beats/min, 8.0 V) (Table 2). It required ≥2.4 V to slow the SR, and the differences before and after SLGP ablation were statistically significant at voltage levels ≥0.3 V (P_1, Table 2). After SLGP ablation, subsequent ablation of ARGP diminished the maximal effect to 9% (153 ± 16 beats/min baseline vs. 139 ± 11 beats/min, 8.0 V) (Table 2). However, the differences before and after ARGP ablation failed to achieve statistical significance at all voltage levels (P_2, Table 2). No additional effect on SR suppression was observed after subsequent ablation of IRGP. To further investigate the direction of innervation (e.g., left vagosympathetic trunk → SLGP → ARGP → SA node vs. left vagosympathetic trunk → ARGP → SLGP → SA node), only ARGP was ablated in 7 animals, which diminished the maximal effect of left vagosympathetic stimulation on SR to 8% (data not shown in Tables). The residual effect (8%) was similar to that after ablation of SLGP and ARGP (9%) (Table 2).

Effects of right vagosympathetic stimulation on VR during AF. Right vagosympathetic stimulation significantly slowed the VR during AF at voltages ≥1.5 V with a maximal effect of 69% (243 ± 27 beats/min baseline vs. 75 ± 86 beats/min, 8.0 V) (Table 3). The SLGP ablation attenuated the maximal effect to 23% (236 ± 28 beats/min baseline vs. 182 ± 59 beats/min, 8.0 V) (Table 3). The differences before and after ablation were statistically significant at voltages ≥1.5 V (P_1, Table 3). Subsequent ablation of the ARGP induced nonsignificant changes (P_2, Table 3), whereas ablation of IRGP eliminated the VR slowing effects, suggesting that the neural pathways followed a direction such as right vagosympathetic trunk → SLGP → ARGP → IRGP or right vagosympathetic trunk → ARGP → SLGP → IRGP. To differentiate which of the 2 pathways was involved, only the ARGP was ablated in 7 other animals. The maximal response was reduced from 67% (264 ± 31 beats/min baseline vs. 87 ± 85 beats/min, 8.0 V) to 26% (249 ± 27 beats/min baseline vs. 185 ± 66 beats/min, 8.0 V) (data not shown in tables), similar to the magnitude of attenuation after SLGP + ARGP ablation (23%) (Table 3). Subsequent ablation of the IRGP also completely eliminated the VR slowing response.

Effects of left vagosympathetic stimulation on ventricular rate during AF. Left vagosympathetic stimulation significantly reduced VR at voltage ≥1.5 V, and VR was reduced by 70% at 8.0 V (235 ± 25 beats/min baseline vs. 66 ± 80 beats/min, 8.0 V) (Table 4). The SLGP ablation attenuated the response, and the maximal effect was only 27% (229 ± 25 beats/min baseline vs. 163 ± 84 beats/min, 8.0 V) (Table 4). Ablation of the ARGP after SLGP ablation produced no additional effect, whereas subsequent ablation of IRGP completely abolished the effects of left vagosympathetic stimulation. To examine the direction of innervation (e.g., left vagosympathetic trunk → SLGP → ARGP → IRGP vs. left vagosympathetic trunk → ARGP → SLGP → IRGP), only ARGP was ablated in 7 other animals, which moderately reduced the maximal effect of VR slowing from

Table 3 Effects of Right Vagosympathetic Trunk Stimulation on Ventricular Rate (beats/min) During Induced AF Before and After SLGP, ARGP, and IRGP Were Sequentially Ablated

	Baseline	0.3 V	0.6 V	1.5 V	2.4 V	3.2 V	4.5 V	8.0 V
Control, n = 10	243 ± 27	242 ± 27	214 ± 61	98 ± 77†	81 ± 86†	78 ± 85†	81 ± 84†	75 ± 86†
SLGP ablation, n = 10	236 ± 28	236 ± 28	233 ± 28	200 ± 66	198 ± 60	200 ± 60	188 ± 61*	182 ± 59*
P_1	NS	NS	NS	<0.01	<0.001	<0.001	<0.001	<0.001
SLGP + ARGP ablation, n = 10	244 ± 26	240 ± 25	240 ± 28	212 ± 65	213 ± 63	203 ± 70	202 ± 62	195 ± 64*
P_2	NS	NS	NS	NS	NS	NS	NS	NS
SLGP + ARGP + IRGP ablation, n = 8	239 ± 33	239 ± 4	238 ± 32	233 ± 31	224 ± 39	221 ± 33	225 ± 31	224 ± 28
P_3	NS	NS	NS	NS	NS	NS	NS	NS

*p < 0.05; †p < 0.01 (compared with baseline).
Abbreviations as in Table 1.

Table 4 Effects of Left Vagosympathetic Trunk Stimulation on Ventricular Rate (beats/min) During Induced AF Before and After SLGP, ARGP, and IRGP Were Sequentially Ablated

	Baseline	0.3 V	0.6 V	1.5 V	2.4 V	3.2 V	4.5 V	8.0 V
Control, n = 10	235 ± 25	218 ± 55	174 ± 75	95 ± 88†	88 ± 87†	83 ± 74†	76 ± 77†	66 ± 80†
SLGP ablation, n = 10	229 ± 25	229 ± 24	223 ± 29	176 ± 84	182 ± 83	176 ± 82	179 ± 82	163 ± 84*
P_1	NS	NS	<0.05	<0.05	<0.05	<0.05	<0.01	<0.01
SLGP + ARGP ablation, n = 10	235 ± 28	231 ± 20	216 ± 50	167 ± 85	162 ± 92*	161 ± 94	163 ± 91	158 ± 96†
P_2	NS	NS	NS	NS	NS	NS	NS	NS
SLGP + ARGP + IRGP ablation, n = 8	240 ± 33	238 ± 20	237 ± 33	233 ± 28	235 ± 29	229 ± 28	228 ± 29	229 ± 28
P_3	NS	NS	NS	NS	NS	<0.05	<0.05	<0.05

*$p < 0.05$; †$p < 0.01$ (compared with baseline).
Abbreviations as in Table 1.

72% (260 ± 27 beats/min baseline vs. 73 ± 54 beats/min, 8.0 V, before ARGP ablation) to 39% (239 ± 22 beats/min baseline vs. 146 ± 82 beats/min, 8.0 V, after ARGP ablation) (data not shown in Tables). Subsequent ablation of the IRGP in these 7 animals further attenuated but did not eliminate the VR response elicited by left vagosympathetic stimulation (16% reduction in VR at 8.0 V, data not shown in Tables). This residual effect (16%) was larger than that of SLGP + ARGP + IRGP ablation (5% reduction in VR at 8.0 V) (Table 4).

Right and left vagosympathetic stimulation on ERP and AF inducibility. Unilateral right and left vagosympathetic stimulation at a voltage level that slowed the SR by 50% in individual animal was selected and applied to the left or right vagosympathetic trunk before and after GP ablation. Right vagosympathetic stimulation shortened the ERP recorded from the right atrium (RA-D,2: 110 ± 24 ms baseline vs. 82 ± 27 ms stimulation; RA-3,4: 112 ± 20 ms baseline vs. 78 ± 32 ms stimulation) (Table 5, top left). The ERPs along the RSPV recording sites also were shortened by right vagosympathetic stimulation (RSPV-D,2: 113 ± 17 ms baseline vs. 80 ± 31 ms stimulation) (Table 5, top left). The window of vulnerability on the right atrium was widened by right vagosympathetic stimulation (RA-D,2: 6 ± 20 ms baseline vs. 38 ± 31 ms stimulation, RA-3,4: 5 ± 20 ms baseline vs. 46 ± 35 ms stimulation) (Table 5, top right), so did the window of vulnerability on RSPV-D,2 (5 ± 16 baseline vs. 32 ± 36 stimulation) (Table 5, top right). Both ERP shortening and window of vulnerability widening of the right atrium and RSPV were eliminated by ARGP ablation. Left vagosympathetic stimulation elicited ERP shortening of the left atrium and LSPV (Table 5, bottom left), which was eliminated by SLGP ablation. Left vagosympathetic stimulation failed to widen the window of vulnerability of the LA and LSPV sites (Table 5, bottom right).

Discussion

In the present study, a stepwise approach was used to systematically investigate the interactions between vagosympathetic trunk (extrinsic cardiac ANS) and GP (intrinsic cardiac ANS). We found that GP function as "integration centers" (1) that integrate the autonomic innervation between extrinsic and intrinsic cardiac ANS because they affect atrial electrophysiology and pathophysiology as indicated by AF inducibility. For instance, IRGP seems to be the integration center for the extrinsic ANS to innervate the AV node as ablation of IRGP completely eliminated the VR slowing response induced by vagosympathetic stimulation. Other investigators have shown that the ARGP and IRGP play a selective role in regulating SA and AV nodal function, respectively (11–14). Our findings do not support these observations, possibly because we implemented a more systematic approach (e.g., multiple stimulation voltages at multiple GP) to explore the autonomic neural network. Moreover, we found that the integration between the extrinsic and intrinsic cardiac ANS is substantially more complicated than previously thought (15). For instance, vagal innervation often travels through multiple GP before reaching the SA and AV node and GP also modulate the contralateral vagosympathetic inputs.

Figure 2A depicts the proposed interactions between vagosympathetic trunks and SA node. The neural pathway (right vagosympathetic trunk → ARGP → SA node) seems to be the main connection between right vagosympathetic trunk and SA node because after SLGP ablation subsequent ablation of ARGP produced further attenuation of SR slowing induced by right vagosympathetic stimulation (Table 1). Ablation of ARGP alone produced similar effect as sequential ablation of SLGP and ARGP. These results also suggest the presence of another neural pathway (right vagosympathetic trunk → SLGP → ARGP → SA node) with the ARGP being the convergent gate before proceeding to the SA node. Similarly, left vagosympathetic trunk modulates the SA nodal function through both SLGP and ARGP (Table 2). The main neural pathway between the left vagosympathetic trunk and the SA node traverses the SLGP and ARGP sequentially before proceeding to the SA node (left vagosympathetic trunk → SLGP → ARGP → SA node) because subsequent ablation of ARGP after SLGP ablation produced minimal additional effects (Table 2) and ablating only the ARGP produced similar effects as sequential ablation of SLGP and ARGP. These data also suggest that ARGP serves as the integration center for both the right and the left vagosympathetic trunks to modulate

JACC Vol. 50, No. 1, 2007
July 3, 2007:61–8

Table 5 Effects of Right or Left Vagosympathetic Trunk Stimulation on ERP (in ms) and WOV (in ms) of Atria and Pulmonary Veins Before and After ARGP or SLGP Ablation (n = 11)

	ERP								WOV							
	RA-D,2		RA-3,4		RSPV-D,2		RSPV-3,4		RA-D,2		RA-3,4		RSPV-D,2		RSPV-3,4	
	BS	RVG-Stim	BS	RVG-Stim	BS	RVG-Stim	BS	RVG-Stim	BS	RVG-Stim	BS	RVG-Stim	BS	RVG-Stim	BS	RVG-Stim
ARGP ablation																
Before	110 ± 24	82 ± 27*	112 ± 20	78 ± 32†	113 ± 17	80 ± 31†	113 ± 14	99 ± 26	6 ± 20	38 ± 31†	5 ± 20	46 ± 35†	5 ± 16	32 ± 36†	0 ± 0	11 ± 26
After	127 ± 22	120 ± 24	115 ± 23	99 ± 25	109 ± 14	96 ± 29	109 ± 11	104 ± 18	0 ± 0	3 ± 10	0 ± 0	15 ± 25*	2 ± 8	16 ± 31	0 ± 0	5 ± 19
p‡	NS	0.01	NS	NS	NS	NS	NS	NS	NS	0.001	NS	0.011	NS	NS	NS	NS
	LA-D,2		LA-3,4		LSPV-D,2		LSPV-3,4		LA-D,2		LA-3,4		LSPV-D,2		LSPV-3,4	
	BS	LVG-Stim	BS	LVG-Stim	BS	LVG-Stim	BS	LVG-Stim	BS	LVG-Stim	BS	LVG-Stim	BS	LVG-Stim	BS	LVG-Stim
SLGP ablation																
Before	107 ± 23	86 ± 24*	105 ± 13	84 ± 22*	108 ± 19	86 ± 25†	94 ± 11	77 ± 20*	4 ± 13	10 ± 22	2 ± 8	8 ± 20	0 ± 0	8 ± 18	0 ± 0	14 ± 23
After	111 ± 17	108 ± 15	106 ± 20	105 ± 16	108 ± 14	97 ± 24	91 ± 10	85 ± 18	0 ± 0	0 ± 0	4 ± 14	0 ± 0	0 ± 0	7 ± 24	0 ± 0	9 ± 22
p‡	NS	0.013	NS	0.015	NS	NS	NS	NS	NS	NS	NS	NS	NS	NS	NS	NS

*p < 0.05; †p < 0.01 (compared with baseline); ‡comparison before and after ARGP or SLGP ablation.
BS = baseline without stimulation; D,2 = electrode pair in close proximity to ARGP (RA-D,2, RSPV-D,2) or SLGP (LA-D,2, LSPV-D,2); ERP = effective refractory period; LA = multielectrode catheters sewn to the left atrium; LSPV = multielectrode catheters sewn to the left superior pulmonary vein; LVG-Stim = left vagosympathetic stimulation; RA = multielectrode catheters sewn to the right atrium; RSPV = multielectrode catheters sewn to the right superior pulmonary vein; RVG-Stim = right vagosympathetic stimulation; WOV = window of vulnerability; other abbreviations as in Table 1.

Figure 2 Interactions Among Vagosympathetic Trunks, ARGP, IRGP, and SLGP on SAN and AVN Function

(A) Modulation of sinus rate by vagosympathetic stimulation. **(B)** Modulation of ventricular rate during atrial fibrillation by vagosympathetic stimulation. **Thick lines** and **thin lines** indicate strong and weak regulatory effects, respectively. See text for details. AVN = atrioventricular node; LVG = left vagosympathetic trunk; RVG = right vagosympathetic trunk; SAN = sinoatrial node; other abbreviations as in Figure 1.

SR, and IRGP seems to play a trivial role in this process. Because SLGP + ARGP + IRGP ablation failed to eliminate the SR slowing response induced by right or left vagosympathetic stimulation, it indicates the presence of other neural pathways between the vagosympathetic trunk and the SA node that bypass these GP.

Figure 2B depicts the proposed interactions between vagosympathetic trunks and the AV node. Ablation of

ARGP after SLGP ablation produced minimal additional effects on VR slowing induced by left vagosympathetic stimulation, whereas ARGP ablation alone produced smaller effects than sequential ablation of SLGP and ARGP. Ablation of IRGP produced the most dramatic response. These observations suggest the presence of a major neural pathway (left vagosympathetic trunk → SLGP → ARGP → IRGP → AV node) and another pathway (left vagosympathetic trunk → SLGP → IRGP → AV node), both converging at the IRGP before proceeding to the AV node. Moreover, ablation of ARGP followed by IRGP ablation produced more residual effects (16%) than SLGP + ARGP + IRGP ablation, suggesting a neural pathway from SLGP to AV node bypassing the IRGP. This pathway may in part account for the observation that ablating only the ARGP produced smaller effects than sequential ablation of the SLGP and ARGP. The main neural pathway between the right vagosympathetic trunk and the AV node traverses SLGP, ARGP, and IRGP sequentially (right vagosympathetic trunk → SLGP → ARGP → IRGP → AV node), as ablation of ARGP induced similar effects as sequential ablation of SLGP and ARGP. Moreover, sequential ablation of ARGP and IRGP completely eliminated VR slowing induced by right vagosympathetic stimulation (data not shown in Tables), suggesting the absence of a pathway directly connecting ARGP to the AV node. These results also indicate that both ARGP and IRGP are the integration centers for both vagosympathetic trunks to innervate the AV node and IRGP is the final converging point.

Because the main purpose of this study was to provide functional evidence for the interactions between the extrinsic and intrinsic cardiac ANS, we did not pursue the exact courses of the neural pathways within the extrinsic and intrinsic ANS, with the understanding that the neural interactions proposed in Figure 2 are by no means complete. Nevertheless, prior work by other investigators (1–5,11–17) provided a wealth of information showing that the heart itself is richly innervated by the ANS. Although the autonomic ganglia are usually concentrated in several areas covered by epicardial fat pads, the axons and small clusters of autonomic ganglia form an extensive interconnecting neural network. We postulate that these interconnections may constitute the neural pathways elucidated in the present study.

Right and left vagosympathetic stimulation and effects on ERP and AF inducibility. The ERP abbreviation and AF inducibility during vagosympathetic stimulation were also modulated by GP. Right vagosympathetic stimulation shortened the ERP and widened the window of vulnerability at the RSPV and right atrial sites. These responses were eliminated by ARGP ablation. Likewise, left vagosympathetic stimulation induced similar ERP shortening at the LSPV and left atrial sites but failed to widen the window of vulnerability, giving the impression that right vagosympathetic stimulation was more arrhythmogenic than left vagosympathetic stimulation despite similar degrees of ERP shortening. These findings are contrary to a widely accepted notion that shortening of ERP by autonomic stimulation serves as an indicator for AF inducibility. A recent report (10) from our group described a measure of AF inducibility using the window of vulnerability defined as the longest S1–S2 minus the shortest S1–S2 at which AF was induced. Concurrent ARGP stimulation widened the window of vulnerability and allowed both late-coupled and early-coupled premature stimulations to initiate AF. Therefore, the window of vulnerability serves as a better indicator of regional autonomic activity and AF inducibility than the ERP. Although a systematic study of AF inducibility by sequentially ablating individual GP was not performed, we showed that ablating certain critical neural elements (e.g., ARGP) in the intrinsic cardiac ANS can eliminate AF inducibility. We postulate that GP in general may be critical elements that facilitate the occurrence of AF in a hyperactive state of the intrinsic cardiac ANS. Because the ARGP is larger in size and closer to atrial myocardium than the SLGP, we postulate that ARGP may play a more active role than the SLGP in the dynamics of AF initiation because of the larger axonal field extending into both atria. Future studies on the distribution and relative abundance of parasympathetic and sympathetic neural elements in the intrinsic cardiac ANS may provide the anatomical basis for the discrepancies in AF inducibility described in this study and the long-term effects of denervation described by others (16).

Patterson et al. (18) showed that both parasympathetic and sympathetic components are required to induce rapid-triggered firing to initiate AF. Therefore, no adrenergic blocker was used in conjunction with vagosympathetic stimulation in this study to avoid suppressing the sympathetic activity and artificially altering the window of vulnerability and AF inducibility. It is also known that vagosympathetic trunks contain sympathetic nerve fibers (19) that can be activated by electrical stimulation of the entire trunk. In the present study, the results acquired at a higher level of stimulation might be confounded by sympathetic activation, particularly after GP, which are known to contain predominantly parasympathetic neural elements, were ablated. However, the magnitude of attenuation of SR and VR slowing would have been even greater without concurrent sympathetic activation, further strengthening the conclusions drawn in the present study.

Clinical implications. Recently, AF ablation targeting the intrinsic cardiac ANS has been shown to improve the success rate for AF ablation (20–22). The intrinsic cardiac ANS, particularly the GP, was ablated either intentionally (20,21) or inadvertently (22). The capability of axonal regeneration after injury has been known for decades, but regeneration of neurons after injury is rare. Thus, AF ablation aiming at autonomic denervation should selectively target the autonomic ganglia (neurons) located within GP to produce long-term denervation and cause minimal myocardial damage. The data from this study showed that ARGP ablation attenuated ERP shortening and window of vulnerability widening induced by right vagosympathetic stimulation, providing additional support for the clinical

efficacy of GP ablation for AF. It is crucial to point out that partial autonomic denervation may increase the incidence of AF as described by Hirose et al. (23). Therefore, an ablation strategy targeting the intrinsic cardiac ANS should be designed so as to avoid partial denervation (mainly the right side) that can accentuate the dispersion of refractoriness across the atria and facilitate AF initiation as shown by the elegant mapping study of Hirose et al. (22) and recently confirmed by Oh et al. (17).

Study limitations. This study was not intended to provide a complete body of knowledge about the complicated interaction between the extrinsic and intrinsic cardiac ANS or the interaction within the intrinsic ANS itself. We selected 3 GP whose human equivalents can be identified and ablated in patients with AF (21) to provide experimental evidence for the hypothesis that external cardiac ANS exerts its influences on SA and AV nodal function and AF inducibility through the intrinsic cardiac ANS. Other potentially important GP such as the GP between the superior vena cava and aortic root (15) and the GP near the ligament of Marshall (24) were not studied for the enormous number of permutations that would have generated in stepwise ablation of GP. The results presented herein may assist future researchers in defining the complex interactions between the extrinsic and intrinsic ANS.

In the present study, vagosympathetic trunks were not decentralized to maintain a more physiological state. We acknowledge that vagosympathetic stimulation may activate the afferent vagal or sympathetic fibers and initiate reflexes that are difficult to quantify. Therefore, all of the experiments in this study were designed in pairs to estimate the contribution of each GP by analyzing the differences in parameters before and after ablation of that GP. We presume that the reflexes activated by vagosympathetic stimulation before and after GP ablation were very similar and that their impact could be minimized by paired analysis. By the same token, potential confounding effects from stimulating the sympathetic nerves could be minimized by paired analysis.

Conclusions

The GP function as the integration centers that modulate the autonomic innervation between extrinsic and intrinsic cardiac ANS, as ablation of SLGP, ARGP, and IRGP markedly altered SR slowing, VR slowing, and AF inducibility with vagosympathetic stimulation. The integration between extrinsic and intrinsic cardiac ANS is substantially more intricate than previously thought. The present study also provides experimental support for the clinical efficacy of GP ablation for AF.

Reprint requests and correspondence: Dr. Sunny S. Po, 1200 Everett Drive, Room TUH6E103, Oklahoma City, Oklahoma 73104. E-mail: sunny-po@ouhsc.edu.

REFERENCES

1. Ardell JL. Structure and function of mammalian intrinsic cardiac neurons. In: Armour JA, Ardell JL, editors. Neurocardiology. 2nd edition. New York, NY: Oxford University Press, 1994:95–114.
2. Yuan BX, Ardell JL, Hopkins DA, et al. Gross and microscopic anatomy of the canine intrinsic cardiac nervous system. Anat Rec 1994;239:75–87.
3. Armour JA, Murphy DA, Yuan BX, et al. Gross and microscopic anatomy of the human intrinsic cardiac nervous system. Anat Rec 1997;247:289–98.
4. Pauza DH, Skripka V, Pauziene N. Morphology of the intrinsic cardiac nervous system in the dog: a whole-mount study employing histochemical staining with acetylcholinesterase. Cells Tissues Organs 2002;172:297–320.
5. Randall WC, Ardell JL. Differential innervation of the heart. In: Zipes DP, Jalife J, editors. Cardiac Electrophysiology: From Cell to Bedside. Philadelphia, PA: Saunders, 1985;137–44.
6. Allessie MA, Rensma PL, Brugada J, et al. Pathophysiology of atrial fibrillation. In: Zipes DP, Jalife J, editors. Cardiac Electrophysiology: From Cell to Bedside. Philadelphia, PA: Saunders, 1990;548–59.
7. Bettoni M, Zimmermann M. Autonomic tone variations before the onset of paroxysmal atrial fibrillation. Circulation 2002;105:2753–9.
8. Scherlag BJ, Yamanashi W, Patel U, et al. Autonomically induced conversion of pulmonary vein focal firing into atrial fibrillation. J Am Coll Cardiol 2005;45:1878–86.
9. Po SS, Scherlag BJ, Yamanashi WS, et al. Experimental model for paroxysmal atrial fibrillation arising at the pulmonary vein-atrial junctions. Heart Rhythm 2006;3:201–8.
10. Zhou J, Scherlag BJ, Edwards J, et al. Gradients of atrial refractoriness and inducibility of atrial fibrillation due to stimulation of ganglionated plexi. J Cardiovasc Electrophysiol 2007;18:83–90.
11. Quan KJ, Lee JH, Geha AS, et al. Characterization of sinoatrial parasympathetic innervation in humans. J Cardiovasc Electrophysiol 1999;10:1060–5.
12. Quan KJ, Lee JH, Van Hare GF, et al. Identification and characterization of atrioventricular parasympathetic innervation in humans. J Cardiovasc Electrophysiol 2002;13:735–9.
13. Carlson MD, Geha AS, Hsu J, et al. Selective stimulation of parasympathetic nerve fibers to the human sinoatrial node. Circulation 1992;85:1311–7.
14. Ardell JL, Randall WC. Selective innervation of sino-atrial and atrioventricular nodes in canine heart. Am J Physiol 1986;251:H764–73.
15. Hirose M, Leatmanoratn Z, Laurita KR, et al. Effects of pituitary adenylate cyclase-activating polypeptide on canine atrial electrophysiology. Am J Physiol Heart Circ Physiol 2001;281:H166–74.
16. Chiou CW, Eble JN, Zipes DP. Efferent vagal innervation of the canine atria and sinus and atrioventricular nodes. Circulation 1997;95:2573–84.
17. Oh S, Zhang Y, Bibevski S, et al. Vagal denervation and atrial fibrillation inducibility: epicardial fat pad ablation does not have long-term effects. Heart Rhythm 2006;3:701–8.
18. Patterson E, Po SS, Scherlag B, et al. Triggered firing in pulmonary veins initiated by in vitro autonomic nerve stimulation. Heart Rhythm 2005;2:624–31.
19. Armour JA, Hopkins DA. Anatomy of the extrinsic effect autonomic nerves and ganglia innervating the mammalian heart. In: Randall WC, editor. Nervous Control of Cardiovascular Function. New York, NY: Oxford University Press, 1984:20–45.
20. Platt M, Mandapati R, Scherlag BJ, et al. Limiting the number and extent of radiofrequency applications to terminate atrial fibrillation and subsequently prevent its inducibility (abstr). Heart Rhythm 2004;1:S11.
21. Scherlag BJ, Nakagawa H, Jackman WM, et al. Electrical stimulation to identify neural elements on the heart: their role in atrial fibrillation. J Interv Card Electrophysiol 2005;13:37–42.
22. Pappone C, Santinelli V, Manguso F, et al. Pulmonary vein denervation enhances long-term benefit after circumferential ablation for paroxysmal atrial fibrillation. Circulation 2004;109:327–34.
23. Hirose M, Leatmanoratn Z, Laurita KR, et al. Partial vagal denervation increases vulnerability to vagally induced atrial fibrillation. J Cardiovasc Electrophysiol 2002;13:1272–9.
24. Kim DT, Lai AC, Hwang C, et al. The ligament of Marshall: a structural analysis in human hearts with implications for atrial arrhythmias. J Am Coll Cardiol 2000;36:1324–27.